sciendo

LATVIAN JOURNAL OF PHYSICS
AND TECHNICAL SCIENCES
2023, N 5

DOI: 10.2478/lpts-2023-0028

SYNTHESIS OF $NaYF_4:Yb^{3+}$, Tm^{3+} NANOCRYSTALS VIA THE THERMAL DECOMPOSITION METHOD USING REFINED SUNFLOWER OIL

L. Smelkovs*, V. Viksna, J. Teterovskis, J. Grube

Institute of Solid State Physics, University of Latvia,
8 Kengaraga Str., Riga, LV-1063, LATVIA
*e-mail: lukass.smelkovs@cfi.lu.lv

In recent years, up-conversion luminescence nanoparticles have attracted significant attention from researchers in fields such as analytical chemistry (for example qualitative and quantitative analysis of metal and non-metal ions) and biomedicine (cancer imaging, drug delivery, treatment, etc.) due to their high rate of emission efficiency, easy surface functionalization, great chemical and thermal and photostability and other favorable properties. $NaYF_4$ in particular has attracted interest of researchers as a host material due to its low phonon energy, thus increasing the efficiency of emission. In this study, the synthesis of $NaYF_4:Yb^{3+},Tm^{3+}$ nanocrystals using the hydrothermal method was successfully carried out. Refined sunflower oil containing oleic acid was used as a solvent instead of analytical grade oleic acid and octadecene-1, reducing the cost of the synthesis. Using semi-quantitative XRD measurement analysis, it was determined that 25.3 % hexagonal β-$NaYF_4:Yb^{3+},Tm^{3+}$ as well as 23.8 % cubic α-$NaYF_4$ nanocrystal crystalline phases were found in the synthesized sample. The sample showed mainly luminescent characteristics typical of hexagonal $NaYF_4:Yb^{3+},Tm^{3+}$ lattice nanoparticles.

Keywords: *$NaYF_4:Yb^{3+}$, Tm^{3+}, refined sunflower oil, thermal decomposition, up-conversion luminescence.*

1. INTRODUCTION

Nanoparticles emitting up-conversion luminescence (UCNPs) are a type of nanoparticles that are able to emit visible and even ultraviolet (UV) light upon excitation by near infrared (NIR) radiation via the anti-Stokes process, where multiple IR photons absorbed by a material are converted into photons with higher energy [1]. $NaYF_4$ nanoparticles in particular have attracted the interest of researchers due to low phonon

energy, resulting in enhanced emission characteristics [2]. Like other UCNPs, they have shown to exhibit properties such as relatively high rate of emission efficiency, great chemical and thermal photostability, low toxicity, easy surface functionalization, and excellent biocompatibility (e.g., with human cells, blood serum). Due to these abilities, the research so far has been primarily focused on biosensing and cancer imaging, drug delivery, virus detection and treatment [3]–[6], as well as quantitative analysis of metal and non-metal ions, inorganic compounds, organic compounds in water, food, saliva and human blood/serum [7]–[12].

In particular, the hexagonal crystalline phase of $NaYF_4$:Yb^{3+},Tm^{3+} several nanoparticle synthesis methods can be found in academic literature. Hexagonal crystalline phase nanocrystals and their synthesis methods are of particular interest, since the hexagonal crystalline phase of $NaYF_4$:Yb^{3+},Tm^{3+} exhibits better up-conversion (UC) luminescence properties as opposed to the cubic crystalline phase [13]–[14].

There are several methods that can be used to synthesize hexagonal $NaYF_4$:Yb^{3+},Tm^{3+} nanoparticles, including co-precipitation, microemulsion, thermal decomposition, combustion synthesis, sol-gel method, and hydro/solvothermal synthesis. Co-precipitation method is useful for creating small nanocrystals. The method is cheap and time-efficient. It is economical, eco-friendly, and needs low (ambient) temperature, which allows for its application in large-scale production to afford nanocrystals with high aqueous solubility.

Moreover, the reaction conditions for precipitation are mild and can be easily adjusted to achieve the desired outcome. The downsides of this method are the synthesized UCNPs need for high temperature calcination and post-annealing, as well as the tendency towards poor/undesired morphology and uneven size distribution. Additional drawback of this method is the formation of hard aggregates, mainly due to the bridging of adjacent particles with H_2O through hydrogen bonds and the corresponding broad capillary forces created during drying. Another synthesis method is thermal decomposition. Its advantages include monodispersed crystals with good morphology and strong up-conversion emission. The disadvantages of this method are fairly difficult synthesis conditions, use of expensive and sensitive metal precursors, as well as generation of toxic byproducts. Sol-gel processing uses cheap precursors, produces nanoparticles with high UC luminescence intensity and may be scaled to industrial levels due to the high crystallinity formed at high annealing temperature. The drawbacks include the necessity of post-heating treatment.

Other issues are considerable particle aggregation, broad particle size distribution, irregular morphology, and insolubility in water. The advantages of microemulsion method are relatively easy operation, the small size of the UCNPs, and the ability for the control of morphology of products by adjusting the dosage of the surfactant, solvent, as well as the aging time. This method, however, usually produces low yield, the scope of analysis is narrow, and sample separation is difficult. A hydro/solvothermal method can also be conducted, in which core-shell-structured nanoparticles are synthesized. The advantages of this method lie in the method ability to produce nanocrystals of desired lattice (cubic, hexagonal) and size fairly consistently, to ensure high purity grade of nanoparticles, which several other methods lack, as well as mild reaction conditions and high reaction activity. Furthermore, it does not require a very exacting operation of the synthesis process. A significant disadvantage is that this method usually requires an autoclave, which means that the growth

of nanocrystals cannot be monitored in real time, and the reaction time is generally long [15]–[20].

The synthesis method employed in this paper is thermal decomposition, where core-shell nanoparticle structure is synthesized. Advantages of the method include monodispersed crystals with good, uniform morphology, high crystal transition strength, easily adjustable and monitorable parameters during crystal growth, as well as strong up-conversion emission. The disadvantages of this method are fairly difficult synthesis conditions, use of expensive and sensitive metal precursors, need for further surface modification for biomedical application, as well as generation of toxic byproducts. [15]–[18], [20], [21]. An outstanding benefit of the core-shell technology is that different rare-earth ions can be confined in different layers to achieve a controllable interaction between the doped ions and their environment, and an additional benefit is improved UC emission [21].

Typically, this synthesis method is done utilizing ocatdecene-1 and oleic acid. Oleic acid is used both as a solvent and a reactant, the polar part of which reacts with nanocrystals when forming the core-shell structure, while octadene-1, being non-polar, is used only as a solvent. In this synthesis, both of these solvents were swapped out for refined sunflower oil (RSO), reducing the cost of the synthesis, since RSO is much cheaper than analytical grade oleic-acid and octadecene-1, reducing the overall cost of the synthesis method, as well as using a much more common and readily available solvent, thus making the industrial production of nanocrystals more feasible, plausible and appealing. Although there has been considerable amount of research in nanoparticle synthesis using sunflower oil [22], to our knowledge, there have been no prior accounts in literature of synthesizing $NaYF_4:Yb^{3+},Tm^{3+}$ using RSO as a solvent via the thermal decomposition method.

2. EXPERIMENTAL

2.1. Synthesis Process

Materials used in the synthesis: 74.7 % Y_2O_3, 25% Yb_2O_3 and 0.3 % Tm_2O_3 for core part of nanoparticles, and 100 % Y_2O_3 for shell up-conversion nanoparticles. Other materials used for synthesis are 37 % hydrochloric acid (HCl), deionized water, refined sunflower oil (RSO), petroleum, cyclohexane, chloroform, methanol, sodium hydroxide (NaOH), and ammonium fluoride (NH_4F).

2.1.1. Shell Synthesis

In the three-necked flask 0.113 g of Y_2O_3 is added and 36 ml of diluted HCl solution (30 ml of deionized water and 6 ml HCl). The flask is then placed in magnetic heated stirrer, and the solution is heated up till it becomes clear. It is then transferred to an oven that is heated to 110 °C, and kept for 24 hours. The following day, the flask is taken out of the oven, and 21 ml of RSO is added. The flask is then placed back in magnetic heated stirrer and is connected to argon gas cylinder, thermometer and water jet pump. Three aeration cycles are done (making vacuum and adding argon 3 times) to get rid of all the oxygen. The solution is heated up to 240 °C and then cooled down to room temperature. In the meantime, methanol solution is prepared. In two

separate containers, methanol solution is made. One contains 0.1 g of NaOH and 10 ml methanol, while the other contains 0.2 g of NH_4F and 10 ml of methanol. Both containers are then placed in ultrasonic bath to mix for approximately 1 hour until everything is dissolved. After that, both methanol solutions are combined and poured in flask, which is at room temperature. Solution is then mixed for 30 minutes, and then three aeration cycles are done. Once all the methanol has evaporated, the solution is heated up to 300 °C, so that nanoparticles can start to form and grow. For 5 minutes, the solution is held at 300 °C, and then cooled down to room temperature. 50 ml of petroleum is added and mixed for 30 minutes. The solution is then poured in centrifuge tubes and placed in a centrifuge at 6000 revolutions per minute (rpm) for 10 minutes. After centrifugation, petroleum with other liquids is poured out and is left with sediments. 20 ml of petroleum is added to each centrifuge tube, and all sediments are dissolved. The solution is then poured back into three-necked flask, mixed for 24 hours more to get more organic byproducts out of the solution. The solution is then added into centrifuge and centrifuged at 6000 rpm for 10 minutes. The petroleum is then poured out and 10 ml of cyclohexane is added to each centrifuge tube. 5 ml of RSO is then added into a beaker and heated up until all of the cyclohexane evaporates. The solution is left to cool down and shell nanoparticles are ready to be injected into synthesized core nanocrystals.

2.1.2. Core Synthesis

Core synthesis is similar to shell synthesis as the only difference is the concentrations of additives. In the three-necked flask 0.201 g of R_2O_3 (R: Y_2O_3, Yb_2O_3, Tm_2O_3) is added with 54 ml of diluted HCl solution (45 ml of deionized water and 9 ml HCl). Solution is heated till it becomes clear and is transferred to the oven that is heated to 110 °C and kept for 24 hours. The next day 31.5 ml of RSO is added to the flask. Methanol solution is made with 0.15 g of NaOH and 12.5 ml of methanol and 0.3 g of NH_4F and 12.5 ml of methanol. The next few steps are done exactly as in shell synthesis. Once the solution has reached 300 °C it is held at that temperature for 2 hours and then shell particles are injected into core structure. The solution cools down to approximately 280 °C once the shell is injected. It is then heated back up to 300 °C and held for an additional hour. Once the solution has cooled down to room temperature, 50 ml of petroleum is added, it is then mixed for 30 minutes. The solution is then centrifuged at 6000 rpm for 10 minutes. Petroleum is then poured out so that the tubes contain only the sediments. 20 ml of chloroform is then added to each centrifuge to dissolve the sediments containing the nanocrystals.

2. RESULTS AND DISCUSSION

3.1. Synthesized Sample Morphology and Fluorescent Property Characterisation

Synthesized sample morphology was studied using Scanning Electron Microscope (SEM) Thermo Scientific Helios UX 5 in scanning transmission electron microscope (STEM) mode. UCNP size analysis was performed using ImageJ soft-

ware. Sample structure was studied using RIGAKU X-Ray diffractometer MiniFlex 600. The measurements were taken at 40 kV and 15 mA with copper X-ray tube.

UC luminescence spectra of synthesized nanoparticles was measured using standard luminescence measurements setup. UC luminescence was excited using Thorlabs L975P1WJ CW laser diode on TCLDM9 - TE-Cooled Mount from Thorlabs. Laser diode input current was controlled using Thorlabs current controller LDC220C, laser diode temperature was controlled using Thorlabs temperature controller TED200C. The laser diode temperature was set so that the radiation emitted by the laser diode coincided with Yb^{3+} absorption maximum at 976 nm. Solution with UCNP was filled into UV fused quartz cuvettes (Thorlabs CV10Q3500F). UC luminescence was collected into the spectrometer Andor Kymera 328i-B1 coupled with Andor iStar CCD camera. All measured UC luminescence spectra were corrected according to the measurement system spectral response.

3.1.1. XRD Measurements

A XRD measurement was carried out determine the crystalline structure of synthesized nanoparticles. Before measurements, samples were dried out to obtain them in powder form. The diffraction peak measurement was compared with ICDD PDF-2 database entries. The results (Fig. 1) show that there are diffraction peaks that correspond to hexagonal crystalline phase β-$NaYF_4$ (PDF 00-028-1192), cubic α-$NaYF_4$ (PDF-01-077-2042), as well as NaCl (PDF 01-071-4661) in halite mineral form. Using semi-quantitative analysis, it was calculated that 50.9 % of the sample contained NaCl in halite mineral form, 23.8 % of the sample contained cubic $NaYF_4$ crystals, while 25.3 % of the sample contained desired lattice hexagonal doped $NaYF_4$ nanocrystals.

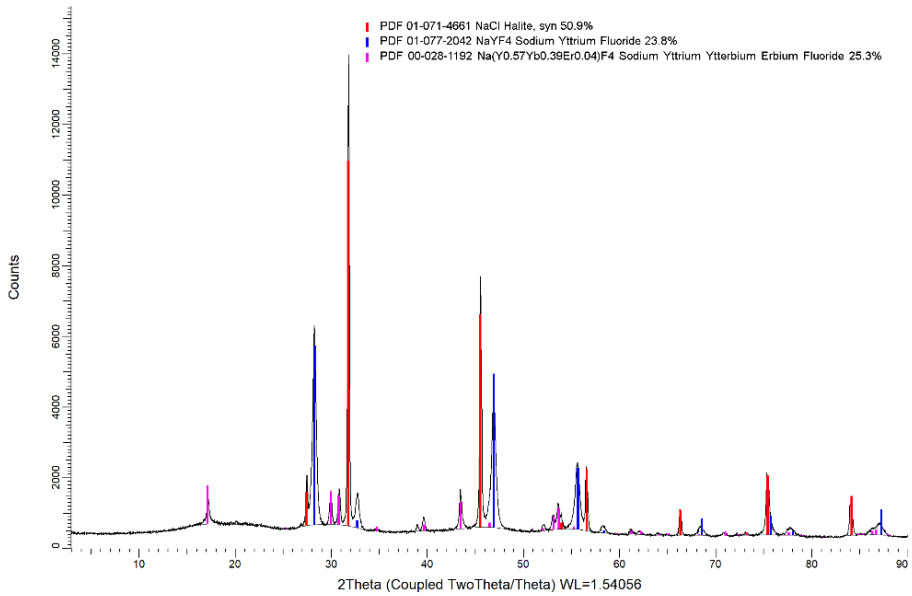

Fig. 1. XRD pattern of synthesized sample. Diffraction maximum positions from databases are given from β-$NaYF_4$ – pink, α-$NaYF_4$, – blue, NaCl in its halite mineral form – red.

To determine the effect of temperature and heating time on the crystalline structure of synthesized sample, additional synthesis was performed. Heating for 10 minutes at 300 °C for core nanoparticles and 5 minutes combined core and shell held at 300 °C, gave only cubic crystalline phase. Increasing the time for core and combined nanoparticles started to change crystalline phase from cubic to hexagonal. Figure 2 shows the presence of these crystalline phases. Our own experimental data and academic literature indicate that α-$NaYF_4$ nanocrystals are first formed, proceed by α → β conversion that occurs via a dissolution / recrystallization process, rather than through oriented aggregation of small α-phase UCNCs [23]. NaCl in the sample is a byproduct of a reaction between lanthanoid chlorides and NaF. It is also plausible to assume that NaCl may have formed due to side reactions with other compounds that are commonly found in RSO, such as linoleic acid, palmitic acid, stearic acid, esters, polyphenols, terpenoids, etc. [24].

3.1.2 STEM Measurements

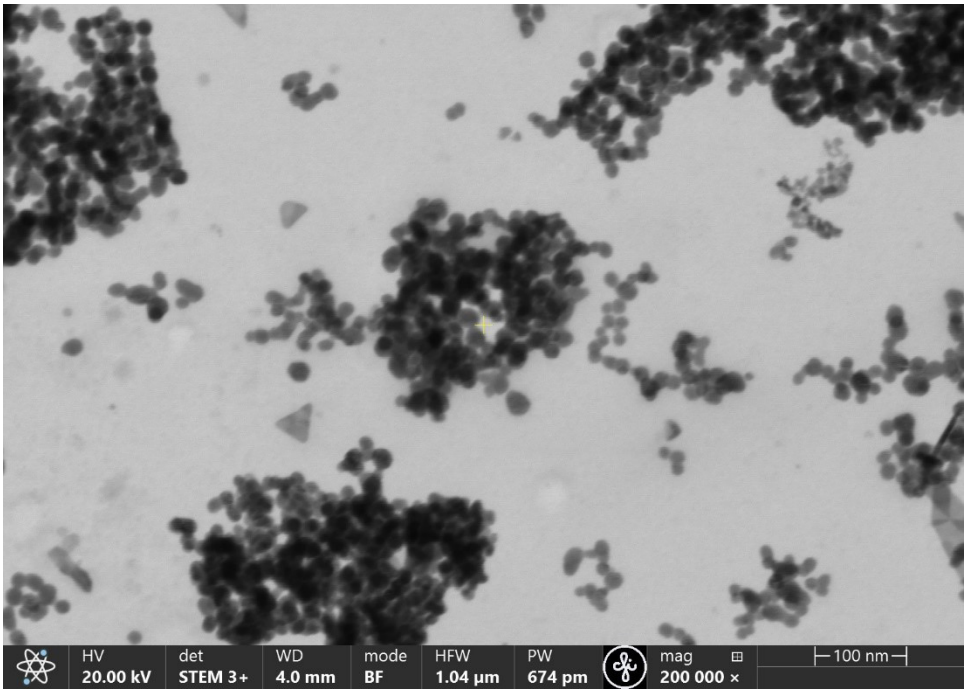

Fig. 2. STEM image of synthesized $NaYF_4$ nanoparticles doped with Yb^{3+},Tm^{3+}.

Using STEM it is possible to determine nanoparticle size and size distribution. Figure 2 shows that nanoparticles are agglomerated. Residual organic material after several rinsing processes can be also observed in Fig. 2, distorting the STEM image. Apart from the base material, there are also some plate-like crystals in the sample, which can be something that has crystallized from the solvent. These were quite resistant to e-beams, so these could be inorganic substances resulting from synthesis. Analysis

of nanoparticle size distribution shows that the mean size of synthesized nanoparticles is 17.2 ± 3.0 nm. STEM measurements allow determining synthesized nanoparticle morphology and size distribution, but not distinguishing core and shell part for nanoparticles in this study. This is explained by the fact that core and shell parts are made from the same base material – $NaYF_4$ only core part is doped with Tm^{3+} and Yb^{3+}, which only slightly affect $NaYF_4$ crystalline structure parameters [25]. Changes that have occurred by dopant introduction into base matrix cannot be detected by STEM measurements. The effect of the shell part on the dimensions of the nanoparticle can be determined by the electron microscopy measurement of nanoparticles obtained at different stages of synthesis processes [23].

3.1.3 Up-conversion Luminescence Measurements

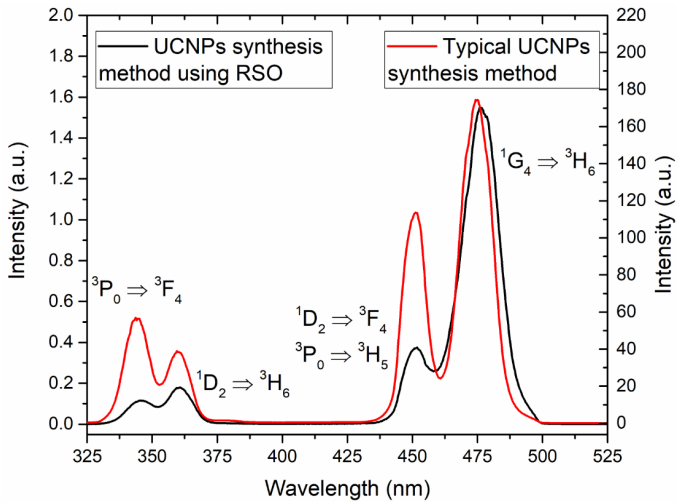

Fig. 3. Black line UC luminescence spectrum of synthesized $NaYF_4$ doped with Yb^{3+}, Tm^{3+} using RSO. Red line shows UC luminescence spectrum $NaYF_4$ doped with Yb^{3+}, Tm^{3+} synthesized with typical synthesis method. All spectra are recorded under 976 nm excitation. Tm^{3+} optical transitions for corresponding up-conversion luminescence bands are shown.

Distinguishing blue Tm^{3+} up-conversion luminescence can be observed with naked eye for synthesized $NaYF_4$:Yb^{3+},Tm^{3+} nanoparticles under excitation with 976 nm. Black line in Fig. 3 shows UC luminescence spectrum in blue and UV spectral regions, with Tm^{3+} luminescence bands in blue (476 nm and 454 nm) and UV (375nm and 340 nm) spectral regions: 476 nm - $^1G_4 - {}^3H_6$, 454 nm ($^1D_2 - {}^3F_4$, $^3P_0 - {}^3H_5$), 361 nm ($^1D_2 - {}^3H_6$) and 345 nm ($^3P_0 - {}^3F_4$) [26]. Other Tm^{3+} UC luminescence bands in red and infrared spectral region can also be observed, but the main focus is on UC luminescence bands in blue and UV spectral regions. Although XRD measurements show that $NaYF_4$ cubic and hexagonal phases coexist in the synthesized sample (23.8 % and 25.3 %, respectively), UC luminescence mainly occurs from $NaYF_4$ hexagonal phase due to higher efficiency of UC process since the data found in the literature indicate that hexagonal nanoparticle UCL is a factor of 10^4 brighter than that obtained from the cubic

phase nanoparticles [13].

For comparison, Fig. 3 also shows UC luminescence spectra (red line) for $NaYF_4$ core / shell nanoparticles doped with Yb^{3+}, Tm^{3+} which are synthesized with typical synthesis method [27]. It is possible to observe differences in the ratios of the different UC luminescence bands and in the overall UC luminescence intensity. Observed differences in UC luminescence spectra can be explained by two facts: (1) In this study, only part of synthesized $NaYF_4$ nanoparticles are in hexagonal phase which emits UC luminescence. This means that there are fewer nanoparticles which can emit UC luminesce. (2) In this study, the mean size of synthesized nanoparticles is 17.2 ± 3.0 nm, while in [27] the mean size of nanoparticles is 33.9 ± 4.6 nm. Smaller nanoparticle size means that energy transfer steps from Yb^{3+} to Tm^{3+} are less likely to occur. As a result, over all UC luminescence intensity will be lower compared to nanoparticles with greater size and Tm^{3+} is less likely to become excited to states with higher energy.

4. CONCLUSIONS

In this study, $NaYF_4$:Yb^{3+},Tm^{3+} nanoparticles (in cubic and hexagonal phase) with the size of 17.2 ± 3.0 nm were synthesized by means of thermal decomposition method using refined sunflower oil (RSO) as a substitute for oleic-acid and octadecene-1 that allowed reducing the overall cost of the synthesis method. Crystalline structure of synthesized nanoparticles was defined by the time of synthesis at 300 °C. During the study, 10 minutes at 300 °C core nanoparticles and 5 minutes combined core and shell held at 300 °C gave only cubic crystalline phase. Increasing the time for core and combined nanoparticles started to change crystalline phase from cubic to hexagonal. Characteristic Tm^{3+} up-conversion luminescence bands in blue and UV spectral regions could be observed under 976 nm excitation.

ACKNOWLEDGEMENTS

The research has been funded by the Latvian Council of Science, project "Up-conversion luminescence photolithography in organic compounds using nanoparticles/photoresist composition", project No. lzp-2019/1-0422.

Institute of Solid State Physics, University of Latvia as the Center of Excellence has received funding from the European Union's Horizon 2020 Framework Programme H2020- WIDESPREAD-01-2016-2017-TeamingPhase2 under grant agreement No. 739508, project CAMART².

REFERENCES

1. Auzel, F. (2004). Upconversion and Anti-Stokes Processes with f and d Ions in Solids. *Chemical Reviews, 104* (1), 139–174. https://doi.org/10.1021/cr020357g
2. Yang, D., Chen, D., He, H., Pan, Q., Xiao, Q., Qiu, J., & Dong, G. (2016). Controllable Phase Transformation and Mid-infrared Emission from Er3+-Doped Hexagonal-/Cubic-NaYF4 Nanocrystals. *Scientific Reports*, *6,* 29871. https://doi.org/10.1038/srep29871

3. Bing-Shuai, Z. H. O. U., Shi-Han, X. U., Song-Tao, H. U., Li-Heng, S. U. N., Jie-Kai, L. Y. U., Rui, S. U. N., … & Biao, D. O. N. G. (2022). Recent Progress of Upconversion Nanoparticles in the Treatment and Detection of Various Diseases. *Chinese Journal of Analytical Chemistry, 50* (2), 19–32. https://doi.org/10.1016/j.cjac.2021.08.003

4. Peng, X., Ai, F., Yan, L., Ha, E., Hu, X., He, S., & Hu, J. (2021). Synthesis Strategies and Biomedical Applications for Doped Inorganic Semiconductor Nanocrystals. *Cell Reports Physical Science, 2* (5), 100436. https://doi.org/10.1016/j.xcrp.2021.100436

5. Xin, N., Wei, D., Zhu, Y., Yang, M., Ramakrishna, S., Lee, O., … & Fan, H. (2020). Upconversion Nanomaterials: A Platform for Biosensing, Theranostic and Photoregulation. *Materials Today Chemistry, 17,* 100329. https://doi.org/10.1016/j.mtchem.2020.100329

6. Escudero, A., Becerro, A. I., Carrillo-Carrión, C., Núñez, N. O., Zyuzin, M. v., Laguna, M., … & Parak, W. J. (2017). Rare Earth Based Nanostructured Materials: Synthesis, Functionalization, Properties and Bioimaging and Biosensing Applications. *Nanophotonics, 6* (5). https://doi.org/10.1515/nanoph-2017-0007

7. Liu, Y., Tu, D., Zheng, W., Lu, L., You, W., Zhou, S., … & Chen, X. (2018). A Strategy for Accurate Detection of Glucose in Human Serum and Whole Blood Based on an Upconversion Nanoparticles-Polydopamine Nanosystem. *Nano Research*, *11* (6), 3164–3174. https://doi.org/10.1007/s12274-017-1721-1

8. Li, Z., Lv, S., Wang, Y., Chen, S., & Liu, Z. (2015). Construction of LRET-Based Nanoprobe Using Upconversion Nanoparticles with Confined Emitters and Bared Surface as Luminophore. *Journal of the American Chemical Society*, *137* (9), 3421–3427. https://doi.org/10.1021/jacs.5b01504

9. Hlaváček, A., Farka, Z., Hübner, M., Horňáková, V., Němeček, D., Niessner, R., … & Gorris, H. H. (2016). Competitive Upconversion-Linked Immunosorbent Assay for the Sensitive Detection of Diclofenac. *Analytical Chemistry*, *88* (11), 6011–6017. https://doi.org/10.1021/acs.analchem.6b01083

10. Chen, H., Tang, W., Liu, Y., & Wang, L. (2022). Quantitative Image Analysis Method for Detection of Nitrite with Cyanine Dye-NaYF4:Yb,Tm@NaYF4 Upconversion Nanoparticles Composite Luminescent Probe. *Food Chemistry*, *367,* 130660. https://doi.org/10.1016/j.foodchem.2021.130660

11. Zuo, J., Wang, W., Zhang, D., Wang, X., Ma, Y., Li, P., ... & Zhang, H. (2022). Ultra-Sensitive Water Detection Based on NaErF4@NaYF4 High-Level-Doping Upconversion Nanoparticles. *Applied Surface Science*, *575,* 151701. https://doi.org/10.1016/j.apsusc.2021.151701

12. Yang, C., Li, Y., Wu, N., Zhang, Y., Feng, W., Yu, M., & Li, Z. (2021). Ratiometric Upconversion Luminescence Nanoprobes for Quick Sensing of Hg2+ and Cells Imaging. *Sensors and Actuators, B: Chemical*, *326*, 128841. https://doi.org/10.1016/j.snb.2020.128841

13. Balabhadra, S., Reid, M. F., Golovko, V., & Wells, J. P. R. (2020). A Comparison of the Yb3+ Absorption and Upconversion Excitation Spectra for Both the Cubic and Hexagonal Phases of NaYF4:Yb3+/Er3+ Nanoparticles. *Optical Materials*, *107*, 110050. https://doi.org/10.1016/j.optmat.2020.110050

14. Krämer, K. W., Biner, D., Frei, G., Güdel, H. U., Hehlen, M. P., & Lüthi, S. R. (2004). Hexagonal Sodium Yttrium Fluoride Based Green and Blue Emitting Upconversion Phosphors. *Chemistry of Materials*, *16* (7), 1244–1251. https://doi.org/10.1021/cm031124o

15. Hong, E., Liu, L., Bai, L., Xia, C., Gao, L., Zhang, L., & Wang, B. (2019). Control Synthesis, Subtle Surface Modification of Rare-Earth-Doped Upconversion Nanoparticles and their Applications in Cancer Diagnosis and Treatment. *Materials Science and Engineering C, 105*, 110097. https://doi.org/10.1016/j.msec.2019.110097

16. Ansari, A. A., & Sillanpää, M. (2021). Advancement in Upconversion Nanoparticles Based NIR-Driven Photocatalysts. *Renewable and Sustainable Energy Reviews, 151*, 111631. https://doi.org/10.1016/j.rser.2021.111631
17. Zhou, J., Liu, Q., Feng, W., Sun, Y., & Li, F. (2015). Upconversion Luminescent Materials: Advances and Applications. *Chemical Reviews, 115* (1), 395–465. https://doi.org/10.1021/cr400478f
18. He, M., Huang, P., Zhang, C., Chen, F., Wang, C., Ma, J., … & Cui, D. (2011). A General Strategy for the Synthesis of Upconversion Rare Earth Fluoride Nanocrystals via a Novel OA/Ionic Liquid Two-Phase System. *Chemical Communications*, *47* (33), 9510–9512. https://doi.org/10.1039/c1cc12886h
19. Dinic, I. Z., Rabanal, M. E., Yamamoto, K., Tan, Z., Ohara, S., Mancic, L. T., & Milosevic, O. B. (2016). PEG and PVP Assisted Solvothermal Synthesis of NaYF4:Yb3+/Er3+ Up-conversion Nanoparticles. *Advanced Powder Technology*, *27* (3), 845–853. https://doi.org/10.1016/j.apt.2015.11.010
20. Mehrdel, B., Nikbakht, A., Aziz, A. A., Jameel, M. S., Dheyab, M. A., & Khaniabadi, P. M. (2022). Upconversion Lanthanide Nanomaterials: Basics Introduction, Synthesis Approaches, Mechanism and Application in Photodetector and Photovoltaic Devices. *Nanotechnology, 33* (8), 082001. https://doi.org/10.1088/1361-6528/ac37e3
21. Min, Y., Ding, X., Yu, B., Shen, Y., & Cong, H. (2023). Design of Sodium Lanthanide Fluoride Nanocrystals for NIR Imaging and Targeted Therapy. *Materials Today Chemistry*, *27*, 101335. https://doi.org/10.1016/J.MTCHEM.2022.101335
22. Pawar, R. V., Hulwan, D. B., & Mandale, M. B. (2022). Recent Advancements in Synthesis, Rheological Characterization, and Tribological Performance of Vegetable Oil-Based Lubricants Enhanced with Nanoparticles for Sustainable Lubrication. *Journal of Cleaner Production*, *378*, 134454. https://doi.org/10.1016/J.JCLEPRO.2022.134454
23. Suter, J. D., Pekas, N. J., Berry, M. T., & May, P. S. (2014). Real-Time-Monitoring of the Synthesis of β-NaYF4:17% Yb,3% Er Nanocrystals Using NIR-to-Visible Upconversion Luminescence. *Journal of Physical Chemistry C*, *118* (24), 13238–13247. https://doi.org/10.1021/jp502971j
24. Gotor, A. A., & Rhazi, L. (2016). Effects of Refining Process on Sunflower Oil Minor Components: A Review. *OCL*, *23* (2), D207. https://doi.org/10.1051/ocl/2016007
25. Sarakovskis, A., Grube, J., Mishnev, A., & Springis, M. (2009). Up-conversion Processes in NaLaF4:Er3+. *Optical Materials*, *31* (10), 1517–1524. https://doi.org/10.1016/J.OPTMAT.2009.02.015
26. Grube, J. (2022). Up-conversion Luminescence Processes in NaLaF4 Doped with Tm3+ and Yb3+ and Dependence on Tm3+ Concentration and Temperature. *Appl. Spectrosc. 76*, 189–198. https://doi.org/10.1177/00037028211045424.
27. Perveņecka, J., Teterovskis, J., Vembris, A., Vītols, K., Tropiņš, E., Vīksna, V. T., … & Grūbe, J. (2023). An Innovative Approach to Photolithography for Optical Recording of High-Resolution Two-Dimensional Structures in a Negative SU8 Photoresist by Activation of Up-conversion Luminescence in Yb3+ and Tm3+ Doped NaYF4 Nanoparticles. *Nano-Structures & Nano-Objects, 33*, 100932. https://doi.org/10.1016/J.NANOSO.2022.100932